Journal of Petroleum Science and Engineering 126 (2015) 26–34

Contents lists available at ScienceDirect

Journal of Petroleum Science and Engineering

journal homepage: www.elsevier.com/locate/petrol

Injectivity errors in simulation of foam EOR

T.N. Leeftink, C.A. Latooij, W.R. Rossen *

Department of Geoscience and Engineering, Delft University of Technology, Room 3.18, 2628CN Delft, The Netherlands

ARTICLE INFO

Article history:
Received 31 October 2013
Accepted 25 November 2014
Available online 4 December 2014

Keywords:
method of characteristics
injectivity
fractional-flow theory
non-Newtonian flow
foam

ABSTRACT

Injectivity is a key factor in the economics of foam enhanced oil recovery (EOR) processes. Poor injectivity of low-mobility foam slows the production of oil and allows more time for gravity segregation of injected gas. The conventional Peaceman equation (1978), when applied in a large grid block, makes two substantial errors in estimating foam injectivity: it ignores the rapidly changing saturations around the wellbore and the effect of non-Newtonian mobility of foam. When foam is injected in alternating slugs of gas and liquid ("SAG" injection), the rapid increase in injectivity from changing saturation near the well is an important and unique advantage of foam injection. Foam is also shear-thinning in many cases. This paper considers the two problems in turn: non-Newtonian effects and foam dry-out.

In studying non-Newtonian effects we use the method-of-characteristics approach of Rossen et al. (2011), which resolves both changing saturations and non-Newtonian rheology with great precision near the wellbore, and compare to conventionally computed injectivity using the Peaceman equation in a grid block. By itself, the strongly non-Newtonian rheology of the "low-quality" foam regime makes a significant difference to injectivity of foam. However, one could estimate this effect using the equation for injectivity of power-law fluids, i.e. without accounting for changing water saturation near the well, without much error.

In SAG processes, however, non-Newtonian rheology is less important than accounting for foam collapse in the immediate near-wellbore region. Averaging water saturation in a large grid block misses this dry-out very near the well and the Peaceman equation grossly underestimates the injectivity of gas. This error is similar in kind to, but much greater than, that in conventional gas-injection EOR. The magnitude of the effect on the overall simulation decreases as the simulation grid is refined around the well; this grid refinement is especially important for simulating foam SAG processes. We illustrate with examples using foam parameters fit to laboratory data.

1. Introduction

Enhanced Oil Recovery (EOR) processes employing gas injection (miscible and immiscible solvent or steam injection) can be very efficient in recovering oil where the gas sweeps. Unfortunately, gas injection has poor sweep efficiency (Lake et al., 2014) because of geological heterogeneity, density differences between gas and oil or water, and viscous instability between the gas and the oil or water it displaces. Foam can address all three causes of poor sweep efficiency (Schramm, 1994; Kovscek and Radke, 1994; Rossen, 1996).

The economics of any EOR process depends on maintaining sufficient injectivity. Injectivity is especially problematic in foam EOR (see e.g., Namdar Zanganeh and Rossen, 2013). Simply injecting a very-low-mobility fluid can force a reduction in injection rate to avoid fracturing the injection well. Unintended fracturing of the injection well has plagued some foam applications in the field (Kuehne et al., 1990; Martinsen and Vassenden, 1999). Moreover, injection rate is crucial to the ability of foam to overcome gravity override of injected gas (Rossen et al., 2010). The good injectivity of a SAG process, in which gas and surfactant solution are injected as alternating slugs, is a major advantage for this injection method in overcoming gravity override (Shan and Rossen, 2004; Faisal et al., 2009; Kloet et al., 2009; Boeije and Rossen, in press). In principle, the best foam process for overcoming gravity override in a homogeneous reservoir is a SAG process with one large slug of surfactant solution followed by one large slug of gas.

Two issues complicate the correct prediction of injectivity in SAG foam EOR processes in reservoir simulation, and in particular injectivity of the gas slug. The first is the reaction of foam to changing water saturation close to the well. Foam dries out and collapses abruptly as water saturation falls below a certain value S_w^* (Khatib et al., 1988; Rossen and Zhou, 1995; Alvarez et al., 2001). This "dry-out effect" means that the mobility of gas increases enormously near the injection well and this greatly increases injectivity. Second, gas in

* Corresponding author. Tel.: +31 15 278 6038.
E-mail addresses: t.n.leeftink@student.tudelft.nl (T.N. Leeftink), c.a.latooij@student.tudelft.nl (C.A. Latooij), w.r.rossen@tudelft.nl (W.R. Rossen).

http://dx.doi.org/10.1016/j.petrol.2014.11.026

Nomenclature

H	reservoir height [m]
k	reservoir permeability [darcy]
k_{rg}^{f}	gas relative permeability [dimensionless]
k_{rw}	water relative permeability [dimensionless]
epdry	STARS foam parameter [dimensionless]
φ	reservoir porosity [dimensionless]
fmmob	reference mobility reduction factor [dimensionless]
FM	foam mobility factor [dimensionless]
S_o	oil saturation [dimensionless]
S_w	water saturation [dimensionless]
S_{wc}	connate water saturation [dimensionless]
S_{wr}	irreducible water saturation [dimensionless]
S_g	gas saturation [dimensionless]
f	fractional flow [dimensionless]
f_w	water fractional flow [dimensionless]
Q	injection rate [m^3/s]
t	time [s]
t_D	dimensionless time [dimensionless]
λ	mobility [$m^2/(Pa\ s)$]
λ_{rt}	total relative mobility [$m^2/(Pa\ s)$]
r	radius [m]
r_w	well radius [m]
r_e	outer radius [m]
P	pressure [Pa]
P_D	dimensionless pressure [dimensionless]
P_w	pressure at well [Pa]
P_{re}	pressure at edge of gridblock [Pa]
n	power-law exponent [dimensionless]
μ	viscosity [Pa s]
μ_g	gas viscosity [Pa s]
μ_w	water viscosity [Pa s]
x	position [m]
x_D	dimensionless position [dimensionless]
C_s	surfactant concentration [dimensionless]
MOC	method of characteristics
SAG	surfactant alternating gas
EOR	enhanced oil recovery

foam is a non-Newtonian fluid, at least in some circumstances (Hirasaki and Lawson, 1985; Falls et al., 1989; Alvarez et al., 2001; Xu and Rossen, 2003; Tang and Kovscek, 2006). Its shear-thinning properties reduce the pressure gradient near the well, which increases injectivity.

The Peaceman equation (1978) is used in most finite-different simulators to describe the difference between injection-well pressure and surrounding pressure in a grid block. It faces various challenges dealing with well placement within the grid block, wellbore orientation, permeability anisotropy, partial penetration of the grid block by the well, large aspect ratio in the dimensions of the grid block, and the effect of a hydraulic fracture (Peaceman, 1983, 1993; Babu et al., 1991; Chen et al., 1995; Mochizuki, 1995; Abacioglu et al., 2009; Dogru, 2010; Ibrahim, 2013). These challenges, and extensions of the equation to meet them, are not the focus of this study. This study addresses errors in the Peaceman equation relating specifically to foam EOR.

This paper addresses the dry-out effect in foam and non-Newtonian mobility in turn. For simplicity we focus on two-phase gas–water flow with foam, and assume that mobile oil has been displaced from the near-wellbore region.

Upon gas injection in a SAG foam process, a Buckley–Leverett shock front forms at the leading edge of the gas bank (Rossen et al., 1999; Shan and Rossen, 2004). At the shock there is an abrupt drop in water saturation and water fractional flow. Figs. A3 and A4 in Appendix A show an example. This front is followed by a two-phase spreading wave that extends back to the well, in which foam dries out and collapses. In total, two regions are present; a spreading wave with two-phase flow, and ahead of it flow of liquid only. In our study foam dries out near the well because of water displacement and flow. Evaporation of water into the gas is another mechanism of dry-out and mobility increase near the well, as examined in other studies of gas injectivity without foam (McMillan et al., 2008; Pickup et al., 2012). We do not consider evaporation here, but evaporation may also be an issue for foam.

Our focus is the near-wellbore area, so we assume that surfactant concentration is uniform and constant in the water phase as a result of earlier surfactant injection. We model injectivity during gas injection in a SAG process in two ways. First we represent the region of interest as a grid block, as in reservoir simulators (Computer Modeling Group, 2006; Schlumberger, 2010; Sharma et al., 2011). The injection pressure is calculated from the Peaceman equation (1978), assuming a cylindrical geometry for a rectangular shaped grid block and uniform properties in the grid block. Second, we use the Method of Characteristics (MOC) to examine saturation and mobility near the well and overall injectivity in the same

region. This approach allows correct representation of shocks within a displacement and resolution of saturations around the well not feasible with finite-difference simulations. We use this analytical theory to check the accuracy of the Peaceman equation. Both models are described in the next section.

Others have examined the effects of non-uniform saturations around the well on injectivity in gas-flooding (McMillan et al., 2008; Mathias et al., 2009; Pickup et al., 2012), non-uniform temperature near the well in schemes to heat the near-wellbore region (Baylor et al., 1990; Fanchi, 1990; Pizarro and Trevisan, 1990; Amit Chakma and Jha, 1992) and precipitation/dissolution waves in CO_2 injection into aquifers (Noh et al., 2007). This is the first study of the effects of saturation variation and foam rheology near the wellbore on foam injectivity. As shown below, the effects can be extreme.

2. Models

2.1. Assumptions

The following assumptions are made for both cases (grid-block calculation using the Peaceman equation and MOC):

(1) All phases are incompressible, as is the reservoir, and components are soluble in only one phase. (2) The reservoir has isotropic and uniform permeability. (3) The surfactant concentration C_s in the aqueous phase is uniform and constant in the region of interest. (4) There are only two phases flowing, though a third, immobile oil phase may be present. Oil saturation S_o is uniform and constant. For simplicity, we assume here $S_o=0$. Appendix A discusses the case of a uniform residual oil saturation. (5) The well radius is r_w. Well skin factor is zero. (6) The reservoir is of uniform height H; the vertical injection well penetrates the entire interval. (7) There are no chemical or biological reactions affecting any of the components. (8) The effect of gravity is negligible in the region of interest. (9) Fluids (in this case, gas) are injected with a constant total volumetric rate Q regardless of injection pressure. (10) Foam properties immediately take their steady-state values corresponding to the local water saturation.

For the first case, in which the region of interest is treated as a grid block, the following assumptions are added to those listed above:

(11a) Uniform saturation in the grid block at all times. (12a) For injection-pressure calculations, the reservoir is represented as a cylinder, which is homogeneous and extends from inner radius r_w, where the fluids are injected, to an open boundary at $r_e=W/2$, where W is the width of the (square) grid block. The Peaceman equation (1978) applies, with the rectangular grid block approximated as a cylinder:

$$P_w - P_{r_e} = \frac{Q}{2\pi H k \lambda_{rt}} \ln\left(\frac{r_e}{r_w}\right) \tag{1}$$

where Q is injection rate, H formation thickness, k horizontal permeability, r_w and r_e radii of injection well and the edge of the grid block, respectively. Total relative mobility λ_{rt} is determined by the average water saturation of the grid block S_w:

$$\lambda_{rt} = \left(\frac{k_{rw}(S_w)}{\mu_w} + \frac{k^f_{rg}(S_w)}{\mu_g}\right) \tag{2}$$

where gas relative permeability k^f_{rg} and viscosity μ_g reflect the effects of foam (see Appendix A).

For the second case where we use the Method of Characteristics, assumptions 1–10 again apply, and in addition

11b. The 1D cylindrical reservoir extends from inner radius r_w, where the fluids are injected, to open outer boundary r_e. Injectivity depends on Darcy's law in incompressible radial flow and the variation of water saturation S_w with radial position. 12b. Dispersive processes, including fingering, capillary diffusion and dispersion are negligible.

The foam model used in this study is described in Appendix A.

2.2. Case 1: Peaceman injectivity in grid block

In this first case the region of interest is represented as a grid block, either 10×10 m^2 or 100×100 m^2, surrounding the well. For easier comparison with the MOC calculations below (specifically, to make comparisons at the same dimensionless time), we assume that the grid block has the volume of a cylinder of radius either 5 or 50 m rather than a rectangular volume.

A material balance on the grid block determines how water saturation changes with time. Gas flows in at flow rate Q, and water flows out at rate ($Qf_w(S_w)$), yielding

$$\frac{dS_w}{dt} = -\frac{Qf_w(S_w)}{H\pi r_e^2 \varphi} \tag{3}$$

with

$$f_w \equiv \left(1 + \frac{k^f_{rg}(S_w)}{\mu_g}\frac{\mu_w}{k_{rw}(S_w)}\right)^{-1}. \tag{4}$$

We express dimensionless time in terms of grid-block pore volumes of gas injected, and dimensionless pressure rise relative to that for water injection into the same size grid block with $S_w=1$, for which total relative mobility $\lambda_{rt}=1/\mu_w=1/(0.001)$ (Pa s)$^{-1}$:

$$t_D = \frac{Qt}{\pi r_e^2 H \varphi} \tag{5}$$

$$P_D = \frac{P_w - P_{re}}{(P_w - P_{re})_{S_w=1}} = \frac{1000}{\lambda_{rt}(S_w)}. \tag{6}$$

We solve Eqs. (3) and (1) for dimensionless pressure rise as a function of time numerically. Details are in Leeftink (2013).

2.3. Case 2: solution using method of characteristics

Buckley and Leverett (1941) first applied fractional-flow theory (or, more generally, the Method of Characteristics, MOC) to a waterflood. Since then it has proved useful in understanding and improving a variety of EOR processes (Pope, 1980; Orr, 2007; Lake et al., 2014). Here we restrict ourselves to an application to two-phase flow, i.e. of gas and water. If an oil phase is present, it is immobile, at residual saturation. The assumptions of the theory are listed above. Even with all its assumptions the theory provides valuable insights and proved sufficiently accurate for analysis of a foam field test in the Snorre Field (Martinsen and Vassenden, 1999).

The application of this theory to foam flow is described in detail elsewhere (Zhou and Rossen, 1995; Rossen et al., 1999; Shan and Rossen, 2004). Key to this method is the fractional-flow function $f_w(S_w)$, (Eq. (4)). On a plot of this function one first identifies the points representing the injection condition, J, and the initial condition, I; see Fig. A3 in Appendix A. In a displacement, saturations between J and I advance through the medium with a dimensionless velocity dx_D/dt_D equal to the slope df_w/dS_w of the fractional-flow function at that saturation. Dimensionless time is defined as in Eq. (5) and dimensionless position in radial flow is

$$x_D = \frac{r^2 - r_w^2}{r_e^2 - r_w^2} \tag{7}$$

where r_w is wellbore radius and r_e is outer radius of the region of interest, either 5 or 50 m in our case.

A single-valued, continuous solution for $S_w(x_D,t_D)$ requires a monotonically increasing slope df_w/dS_w from point J to point I on the $f_w(S_w)$ plot. Otherwise, shocks, i.e. discontinuities in S_w, occur. A material balance on water or gas gives the conditions which have to be satisfied by the shock. Specifically, the shock velocity is equal to the slope of the line linking points on the $f_w(S_w)$ plot upstream and downstream of the shock. The shock velocity must also satisfy the condition of monotonically increasing velocity from the J to I. Details of the method are in the references above.

The results can be plotted in a dimensionless time–distance diagram (see Fig. A4 in Appendix A), which shows the advance of the characteristics of fixed S_w through the porous medium. Local mobilities along the characteristics plotted in Fig. A4 are those for the S_w values with the given slope df_w/dS_w on the $f_w(S_w)$ curve.

To obtain the rise in injection pressure, one must first convert $S_w(x_D)$ to $S_w(r)$ (Eq. (7)) and then integrate for pressure from outer radius r_e to wellbore radius r_w using Darcy's law:

$$\frac{\partial P}{\partial r}=\frac{-Q}{2\pi rHk\lambda_{rt}(S_w(r))}. \tag{8}$$

We carry this integration out numerically; details are in Leeftink (2013).

The advantages of the fractional-flow approach are twofold. First, the saturations with extremely low mobility (Fig. A2), that are skipped over in the shock, are excluded from the calculation. As shown below, the appearance of these saturations in finite-difference calculations leads to orders-of-magnitude errors in the estimated mobility near the well. Second, one can resolve the variation of saturation behind the shock with far greater precision than is feasible with finite-difference simulation. In our calculations, for instance, we resolve the region behind the shock into over 100 separate values of water saturation. In effect, when the shock has traveled 50 m we resolve saturations on a scale of cm.

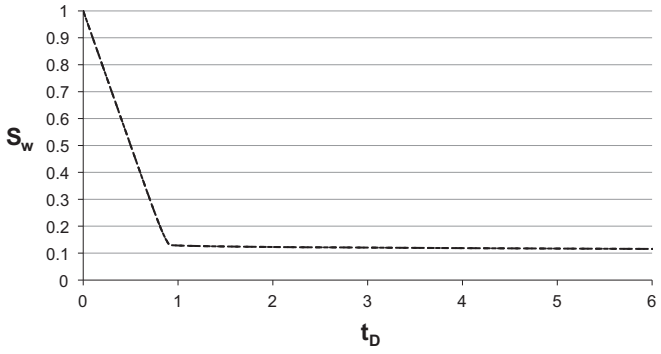

Fig. 1. Water saturation in the grid block as a function of dimensionless time t_D for the case of uniform saturation in the grid block and injectivity calculated with the Peaceman equation. The plot is the identical for 10-m-wide and 100-m-wide grid blocks.

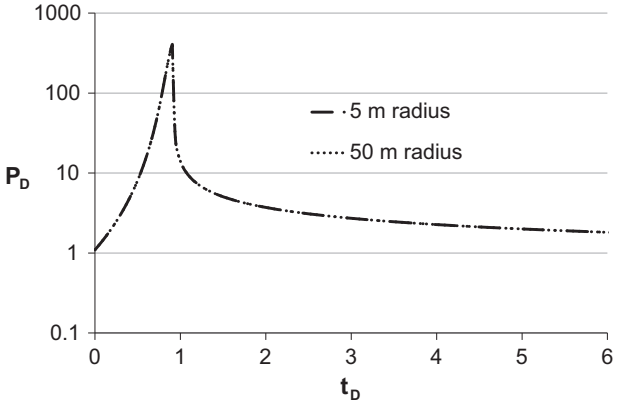

Fig. 2. Dimensionless injection pressure as a function of dimensionless time calculated using Fig. 1 and the Peaceman equation. The plot is the identical for 10-m-wide and 100-m-wide grid blocks.

3. Results

3.1. Effect of foam dryout

3.1.1. Peaceman injectivity in a grid block

Fig. 1 shows water saturation in the grid block as a function of dimensionless time t_D. The plot is the same for both grid-block sizes as a function of dimensionless time. Fig. 2 shows dimensionless injection pressure as a function of dimensionless time. Again, the plot is the same for both grid-block sizes, because injection pressure is dimensionalized by that required to inject water at the same rate with 100% water saturation in the grid block; thus the different ratio of wellbore to grid-block radius (Eqs. (1) and (6)) affects both cases identically. Although the period of low injectivity (large P_D) appears brief in Fig. 2, if injection pressure were limiting rather than rate, injection rate would slow down by a factor of several hundred at the peak in P_D. As a result, the period

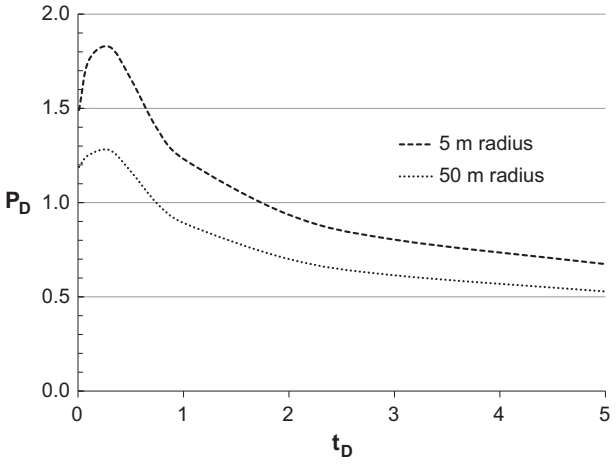

Fig. 3. Dimensionless injection pressure as a function of dimensionless time based on the MOC solution for the two grid-block sizes.

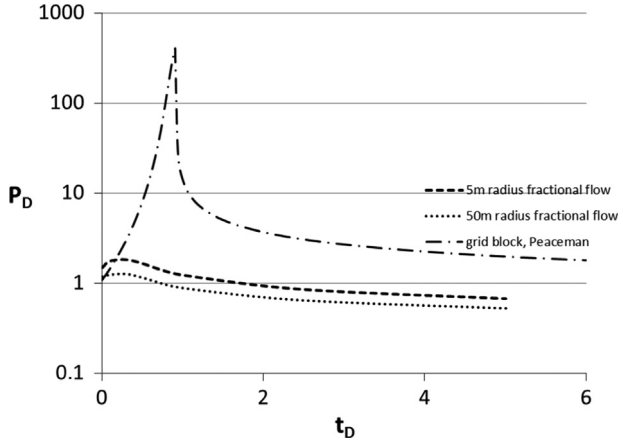

Fig. 4. Comparison of dimensionless injection pressure computed using the Peaceman equation and the solution using the MOC, which accounts for lower water saturation near the well.

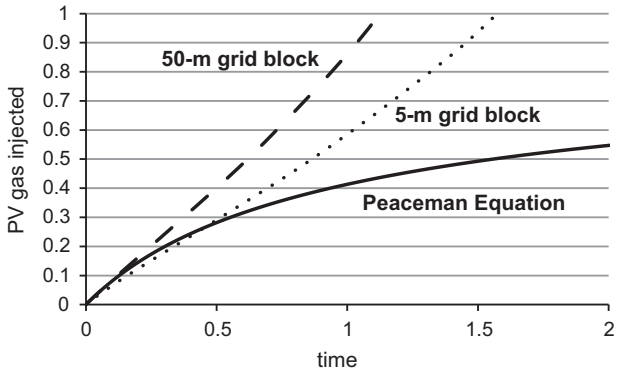

Fig. 5. Cumulative injection in terms of grid-block pore volume of gas injected: MOC solution for 10-m and 100-m grid blocks and Peaceman equation (which gives same solution for either grid-block size). One unit of time here represents the time it would take to inject one grid-block pore volume of water with 100% water saturation in the grid block.

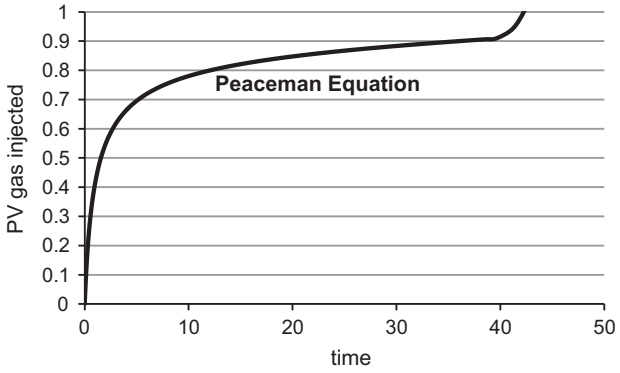

Fig. 6. Extended plot of behavior computed with Peaceman equation (Fig. 5) for longer times.

of low injectivity would be greatly prolonged, as discussed further below.

3.1.2. Solution using method of characteristics

Fig. 3 shows dimensionless injection pressure as a function of dimensionless time for the 10-m and 100-m-wide regions calculated using the MOC. The plots differ because the effect of greater mobility near the wellbore is different for the two cases. For the 100-m wide grid block the near-wellbore region dries out in a smaller faction of the time it takes to inject a pore volume of gas. For gas injection in SAG, injectivity is worst shortly after the start of gas injection (Boeije and Rossen, in press). With increasing time mobility rises near the well (Fig. A4) and injectivity increases.

Fig. 4 compares P_D calculated using the Peaceman equation and assuming uniform water saturation in the grid block with that calculated using the MOC for the two grid-block sizes. For a short time, injectivity is less than estimated using the Peaceman equation, but soon, and for the rest of the period of gas injection, the Peaceman equation grossly underestimates injectivity. The comparison would be more extreme than shown here if we had used a foam model where foam collapses completely at the well; see Appendix A.

Injectivity is so greatly underestimated by the Peaceman equation in a grid block because S_w in the grid block must pass through all the extremely low mobilities between the injected and initial saturations (Fig. A2). In reality, upon gas injection there is a shock front past the saturations of lowest mobility, as illustrated by the MOC solution. Everywhere throughout the foam bank in Fig. A4 the mobility is at least 93 times greater than at its minimum in Fig. A2.

In addition, the MOC recognizes the impact of extremely large mobilities near the injection well (Fig. A4 and Eq. (8)). As calculated with the MOC, the total pressure drop through the foam bank in a SAG process in radial flow is nearly constant (Boeije and Rossen, in press). Therefore, at short times, the injection pressure calculated with the MOC exceeds that with the Peaceman equation: it includes both the foam bank and the water bank in front of it. At later times, as the foam front expands, the Peaceman equation ascribes extremely low mobility to the entire grid block (Fig. A2) while the MOC correctly accounts for the shock and increasing mobility near the well.

3.1.3. Discussion

If injection pressure is fixed rather than injection rate, Figs. 2 and 4 greatly understate the injectivity error with the Peaceman equation in a grid block that is assumed to have uniform saturation. If injection pressure is fixed, then injection rate scales with $(1/P_D)$, and the advance of physical time scales like the integral of (P_D) with respect to t_D. The physical time required to inject a grid-block pore volume of gas is shown in Figs. 5 and 6. A unit of time on these plots corresponds to the time it would take to inject one grid-block pore volume of water with 100% water saturation in the grid block. It takes about 42 time units to inject a grid-block pore volume of gas as calculated using the Peaceman equation (for either grid-block size), compared to 1.57 and 1.12 time units for 10-m or 100-m-wide grid blocks, calculated with the MOC.

The effects are similar in origin, but much larger in magnitude, than those previously shown by McMillan et al. (2008) and Pickup et al. (2012) for gas injection without foam. In the example of Pickup et al. the minimum in mobility at intermediate water saturations is four times lower than at the endpoints. With foam (Fig. A2), it is between three and four orders of magnitude lower. In Pickup et al., evaporation of water raises mobility by another factor of about 15 very near the well. In our case, allowing for complete foam collapse at the well would raise mobility there by about another order of magnitude, as discussed in Appendix A. Allowing for water evaporation, however, would have relatively little effect in our model (Appendix A), because gas relative permeability is nearly 1 at irreducible water saturation.

Our results are scaled to pressure difference between the injection well and the surrounding grid block and to the time required to inject one grid-block pore volume of gas. Refining the simulation grid around the well would reduce the duration of the period of greatest errors, on the time scale of injecting a reservoir or pattern pore volume of gas. It would reduce the magnitude of the error also, because the near-well pressure difference would be a smaller portion of the overall injection pressure rise. Since the immediate vicinity of the injection well is so important to injectivity, however, the magnitude of the error would remain substantial unless the grid were refined to an extraordinary extent near the injection well.

3.2. Effect of non-Newtonian viscosity

The Peaceman equation (Eq. (1)) assumes both uniform saturations in the grid block containing the injection well and Newtonian mobility at that saturation. Shear rates vary greatly within the injection-well grid block. Lake et al. (2014) gives an equation for the injectivity of a non-Newtonian power-law fluid at uniform saturation. Sharma et al. (2011) describe a method to adjust the parameters of the Peaceman equation on an ad-hoc basis to account for non-Newtonian mobility in the near-wellbore region.

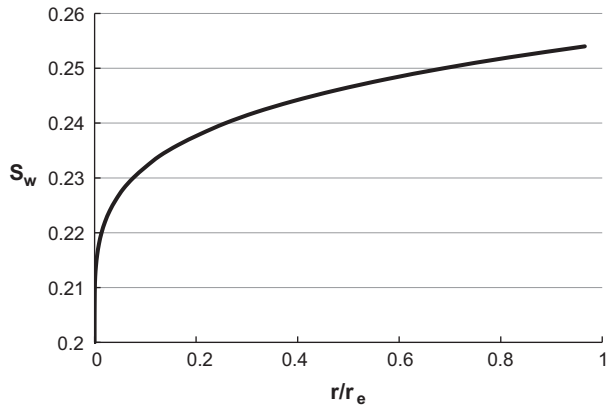

Fig. 7. Water saturation around the well at dimensionless time $t_D=10$, long after the shock has passed beyond the region of interest for the case of non-Newtonian foam; 10-m-wide grid block.

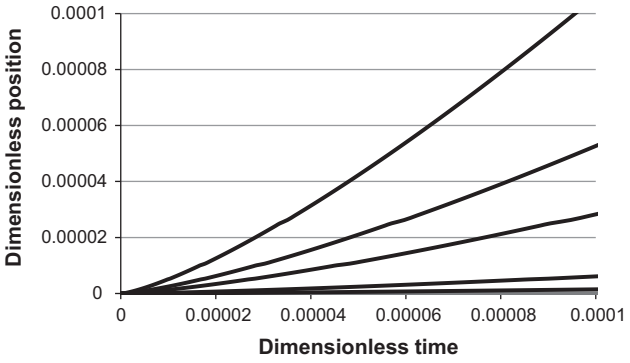

Fig. 8. Characteristics in the spreading wave for gas injection in a SAG process using non-Newtonian foam; water saturation is uniform and constant along each curve. Results from Rossen et al. (2011).

In reality, both effects occur simultaneously: saturation varies with position and time near the well, and mobility at each position may be a non-Newtonian function of superficial velocity at that position. Here we address both issues; for simplicity we exclude the dry-out effect that is the focus of Section 3.1.

Rossen et al. (2011) describe a method for modeling 1D dynamic two-phase displacements with non-Newtonian phase viscosities using the MOC. Unlike the model in Section 3.1, illustrated in Fig. A4, for non-Newtonian fluids the characteristics are curved. Therefore computation of the velocity of the shock front at the leading edge of the foam bank is complex. Rossen et al. show that, for SAG injection, a simple numerical solution using the MOC is possible behind the shock front, i.e. in the near-wellbore region. Thus the method applies only after the shock has left the near-well region, i.e. for dimensionless times greater than about 1 (see slope of shock in Fig. A3). Although the method employs a numerical solution of equations derived from the MOC, these equations can be solved to an arbitrary level of precision (e.g., to the cm scale or below), much more accurately than is feasible with conventional simulation. To simplify the model and focus on non-Newtonian effects, Rossen et al. (2011) exclude the effect of water saturation on foam stability, specifically the abrupt collapse of foam at a limiting water saturation S_w^* described in Section 3.1 above. Thus their study includes the simultaneous effects of changing water saturation and non-Newtonian viscosity, but it excludes by far the largest effect of changing water saturation in a SAG process, the dry-out effect. In a SAG process foam is in the "high-quality" regime dominated by dry-out (Zhou and Rossen, 1995; Shan and Rossen, 2004); rheology in this regime can be non-Newtonian (Osterloh and Jante, 1992; Alvarez et al., 2001), but modeling this effect would require making S_w^* a function of superficial velocities. This is allowed in the current STARS foam simulator (Coombe, 2012) but is not frequently used in simulation.

In the foam model of Rossen et al. (2011), gas mobility is reduced by foam by a factor that is independent of water saturation but depends on total superficial velocity like a power-law fluid with power-law exponent ½. In addition, mobility depends on water saturation because the relative permeabilities of water and gas depend on water saturation. Values of mobility below correspond to an "effective viscosity" of foam (inverse mobility relative to that of water in single-phase flow) of 24–530 cp. Our focus is not on the magnitude of the rise in injection pressure, which is extraordinary given the low mobility of the foam here, but on the effect of non-Newtonian foam behavior on it. Details of the foam model are in Appendix B.

Rossen et al. (2011) note that an important implication of this model is the effect on injectivity, but they do not calculate injectivity. In this paper we use the results of Rossen et al. for water saturation as a function of time and radial position to determine injectivity for a shear-thinning foam in a SAG process. We integrate for pressure around the well numerically using the positions of the characteristics at the given time, as in Eq. (8), but with λ_{rt} dependent on both S_w and position r. Details of the calculations are in Latooij (2012). The definitions of dimensionless time and injection pressure are the same as in Eqs. (5) and (6). As above, the wellbore radius is 0.1 m, and the outer radius is either 5 or 50 m. For a radius of 5 m, Fig. 7 shows water saturation around the well at a dimensionless time $t_D=10$. Fig. 8 shows the curved characteristics behind the shock; as in the MOC for Newtonian fluids, saturation is uniform and constant along each characteristic.

3.2.1. Results: effect of non-Newtonian viscosities

We compute injectivity at two times, one shortly after the shock at the leading edge of the foam bank has left the region of interest ($t_D=1$), and again at 10 times this time ($t_D=10$). For a 10-m wide grid block (outer radius 5 m), at $t_D=1$, the dimensionless injection pressure P_D is 87, reflecting the extremely strong foam assumed in this section (Appendix B). If however one used the Peaceman equation with the total relative mobility equal to that at $r=5$ m at this time, the dimensionless rise would have been 210, i.e. 2.41 times larger. Ten times later, at $t_D=10$, the dimensionless rise in injection pressure is 83, again reflecting an extremely strong foam. If however one used the Peaceman equation with the total relative mobility equal to that at $r=5$ m, the dimensionless rise would have been 190, i.e. 2.29 times larger.

One can distinguish the effects of shear-thinning rheology and changing water saturation near the well as follows. First consider the effect of non-Newtonian (shear thinning) rheology alone. In this case we allow that the effective viscosity changes with radial distance, but assume S_w is uniform throughout the entire region and is equal to its value at the well, i.e. 0.2. The total relative mobility λ_{rt} then depends only on radial position (Eq. (A3)). At the well ($x_D=0$) $\lambda_{rt}=42.23$ $(\text{Pa s})^{-1}$ (an effective viscosity of 23 cp) whereas at the outer radius $\lambda_{rt}=5.97$ $(\text{Pa s})^{-1}$ (effective viscosity 167 cp). The total relative mobility is a factor of 7 lower at the wellbore compared to that at $r=5$ m. As in the previous paragraph, injectivity is over twice as large as that estimated using the mobility at the outer radius.

Next, allow for nonuniform water saturation but not non-Newtonian rheology. At $t_D=1$, $S_w=0.31$ at $r=5$ m and $S_w=0.2$ at the wellbore. Excluding the non-Newtonian effects, the difference in total relative mobility at these two saturations is only 25%. At $t_D=10$, the difference in mobilities is about 13%. Thus, in this case, with

foam dry-out excluded, the effect of changing water saturation near the well is much less important than shear-thinning viscosity.

These results show that, although the changing water saturation does have an impact on injectivity in this model (13–25%), the effect of shear-thinning rheology on injectivity is much greater (i.e., by a factor of more than 2) and is therefore the more important effect.

Moreover, as grid-block size increases, the effect of shear thinning on injectivity increases. For a 100-m-wide grid block (outer radius 50 m), at $t_D=1$ dimensionless rise in injection pressure is 183. If however one used the Peaceman equation with the total relative mobility equal to that at $r=50$ m, the dimensionless pressure rise would have been 618, i.e. 3.38 times larger. At $t_D=10$, the dimensionless rise in injection pressure is 177. If however one used the Peaceman equation with the total relative mobility equal to that at $r=50$ m, the dimensionless rise would have been 576, i.e. 3.26 times larger. As with the 10-m wide grid block, the effect of S_w alone in this case is much smaller: about a 17% difference in mobility at $t_D=1$, and 9% at $t_D=10$. The total relative mobility at the injection wellbore is 22 times greater than that at 50 m for both $t_D=1$ and 10.

Although in this case the effect of dry-out is much greater than that of non-Newtonian mobility, the effect of non-Newtonian mobility is still significant; ignoring it would lead to significant errors in computed injectivity.

Accounting for the effect of non-Newtonian mobility on injectivity would be more important for processes of continuous foam injection than for the SAG example shown. This is especially true if the injected foam is in the low-quality regime (Osterloh and Jante, 1992; Alvarez et al., 2001; Boeije and Rossen, 2013), which is expected to be strongly shear-thinning. During foam injection foam does not dry out and collapse near the injection well, so accounting for non-uniform water saturation is not so crucial to injectivity. In such a case the approach of Sharma et al. (2011) or the equation of Lake et al. (2014), which accounts for non-Newtonian mobility but not for changing water saturation, would suffice to describe injectivity.

4. Conclusions

The following conclusions relate to the dry-out effect on foam and foam injectivity:

(1) In simulation of gas injection in SAG processes, the Peaceman equation, combined with an assumption of uniform saturation in the injection-well grid block, can lead to a massive underestimation of true gas injectivity. If injection pressure is limiting, the period of incorrectly calculated poor injectivity can last for long times. In our example, using the Peaceman equation, the injection-well grid block at one point experiences mobility (Fig. A2) almost 100 times lower than that anywhere within the foam bank (Fig. A4).

(2) These results are expressed in dimensionless time based on grid-block pore volume. Reducing grid size around the injection well would reduce the duration and magnitude of the effect on the reservoir scale, at the price of slower simulator execution. Therefore grid resolution around injection wells is an extremely important issue in modeling SAG foam EOR processes.

(3) The foam model used here assumes (Fig. A1) that gas mobility is reduced by over a factor of 10 even at irreducible water saturation S_{wr}. If instead foam collapsed completely at S_{wr} and gas mobility at the well were 10 times greater, the contrast between true behavior and that simulated using the Peaceman equation would be even greater.

The following conclusion relates to the effect of non-Newtonian foam behavior and injectivity:

(4) Non-Newtonian foam mobility is important to foam injectivity. In the example shown, the actual injectivity is about 2.3 and 3.3 times lower than that which would be estimated using the Peaceman equation and the mobility at the outer radius, for 10-m and 100-m grid blocks, respectively. If one excludes the dry-out effect, then the effect of changing saturation on this result is relatively small, however. This suggests that the approach of Lake et al. (2014) or Sharma et al. (2011), which do not account for nonuniform saturations, suffices to describe this effect for processes of foam injection, in which dry-out does not play the crucial role it plays in SAG injection.

Acknowledgment

A version of this work was presented at the 17th European Symposium on Improved Oil Recovery, sponsored by the EAGE, St. Petersburg, Russia, 16–18 April 2013.

Appendix A. Foam model used in study of effect of dry-out

In the absence of foam we use the following relative-permeability functions for water and gas:

$$k_{rw}=0.6822\left(\frac{S_w-0.05}{0.90}\right)^{2.6844} \tag{A1}$$

$$k^o_{rg}=0.8649\left(\frac{0.95-S_w}{0.90}\right)^{2.2868} \tag{A2}$$

where the superscript o indicates that this is the relative permeability in the absence of foam. Water and gas viscosities 1.0 and 0.02 cp (0.001 and 0.00002 Pa s), respectively. With foam, the water relative-permeability function and viscosity are not altered but gas mobility is greatly reduced (Rossen, 1996). Here we use the foam model in STARS™ (Cheng et al., 2000), in which the effect of foam is represented by an alteration in gas relative permeability:

$$k^f_{rg}=\frac{k^o_{rg}(S_w)}{1+fmmob\left(0.5+(\arctan(epdry\times(S_w-fmdry)))/(\pi)\right)}. \tag{A3}$$

Parameter *fmmob* is the reduction in gas mobility for full-strength foam, in the "low-quality" or wet regime, *fmdry* the water saturation at the transition to the "high-quality regime," where foam dry-out dominates behavior, and *epdry* is a parameter that governs the abruptness of this transition. Here we choose *fmmob*=34,000, *fmdry*=0.13, and *epdry*=10,000. These values are similar to those Cheng et al. (2000) and Rossen and Boeije (2013) derived from coreflood data.

Fig. A1 shows gas and water relative-permeability functions with these parameters, and Fig. A2 shows total relative mobility λ_{rt} (Eq. (2)) as a function of water saturation for those parameters. Total relative mobility in Fig. A2 is inversely related to effective viscosity of foam; $\lambda_{rt}=10$ corresponds to an effective viscosity of 100 cp. Fig. A3 shows the fractional-flow curve (Eq. (4)) for this foam model, along with the shock at the leading edge of the foam bank, and Fig. A4 shows the time-distance diagram for the process, with total relative mobilities marked in for several characteristics.

Fig. A2 also shows the saturation just upstream of the shock formed during gas injection in a SAG process. The deep minimum in λ_{rt} with foam is Fig. A2 disappears into the shock formed during gas injection in a SAG process. For comparison, Fig. A2 also shows total relative mobility for gas–water flow without foam. Without foam, total relative mobility λ_{rt} lacks the deep minimum of the foam curve. This minimum is a major reason why the Peaceman

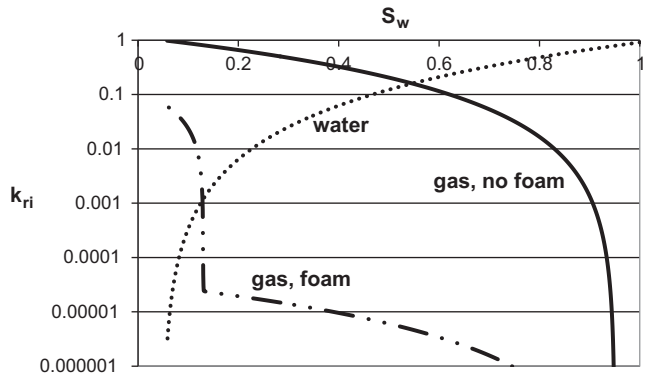

Fig. A1. Gas and water relative-permeability functions for the study of foam dry-out.

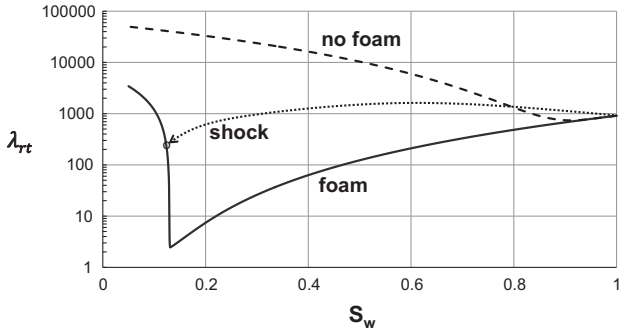

Fig. A2. Total relative mobility of foam (Pa s)$^{-1}$ as a function of water saturation for the study of foam dry-out (solid line). Also shown, total relative mobility for a gas–water displacement without foam, and the jump at the shock at leading edge of gas bank in a SAG foam process. During gas injection, all saturations between $S_w=1$ and the leading edge of the shock disappear into the shock.

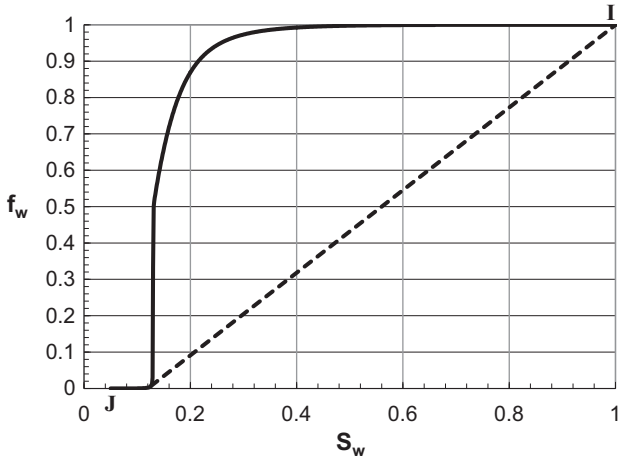

Fig. A3. Fractional-flow function for the study of foam dry-out, with initial state I, injection state J, and shock front at leading edge of gas bank drawn in (dashed line).

equation so greatly underestimates injectivity during gas injection in a SAG process.

Fig. A2 shows that even at irreducible water saturation $S_{wr}=0.05$ gas mobility is reduced by a factor of more than 10 by foam according to this model (cf. Fig. A1). For single-phase gas flow (at $S_w=S_{wr}=0.05$), $\lambda_{rt}=43{,}250$. One expects (Khatib et al., 1988; see also Rossen et al. (2014)) that foam has collapsed at the large capillary pressure at S_{wr}. If the model represented complete collapse, mobility at the wellbore would be 43,250 instead of 4301 as in Fig. A4. The failure of the foam model in STARS to give complete

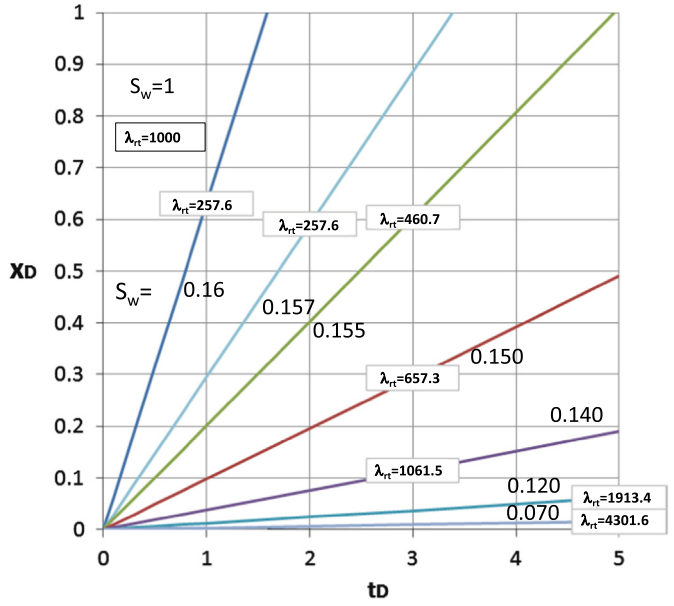

Fig. A4. Time–distance diagram for gas injection in study of foam dry-out. Boxed values are total relative mobility (Pa s)$^{-1}$ for the given characteristic, except (upper left) for 1000, the total relative mobility of the initial state (to the left of the steepest characteristic, which is also the shock front). The other numbers next to the characteristics are the water saturation along each characteristic.

foam collapse at S_{wr} has a large impact on mobility in SAG displacements (Namdar Zanganeh et al., 2011), and, as shown here, on injectivity.

If one assumed the presence of a fixed residual oil saturation, the relative permeabilities in Eqs. (A1) and (A2) would both be reduced, but the deep minimum in λ_{rt} in Fig. A2 would remain. The quantitative results of the model would change somewhat, but the overall conclusions would be unchanged.

Appendix B. Foam model used in non-Newtonian injectivity calculations

In this case we take the relative permeabilities used by Rossen et al. (2011), i.e.

$$k_{rw}=0.2\left(\frac{S_w-0.2}{0.6}\right)^{4.2} \tag{B1}$$

$$k^o_{rg}=0.657\left(\frac{0.8-S_w}{0.6}\right)^{1.3}. \tag{B2}$$

Water and gas viscosities in the absence of foam are 0.001 and 0.00002 Pa s as in the dry-out study. Foam does not affect water relative permeability or viscosity, but does greatly affect gas mobility. It is equivalent to describe this effect as an effect on relative permeability or viscosity. Described as an effect on gas relative permeability we use

$$k^f_{rg}=\frac{k^o_{rg}(S_w)}{55{,}000(r/500)^{(1-n)/2}}=\frac{0.657((0.8-S_w)/0.6)^{1.3}}{55{,}000(r/500)^{(1-n)/2}}. \tag{B3}$$

This corresponds to a foam with extremely large mobility reduction (by a factor of 55,000, which is similar to the model fit of Cheng et al. (2000) to laboratory data without oil) at a radial distance of 500 m. The mobility reduction scales like a power-law

fluid with exponent n for shorter distances. We assume a power-law exponent of ½. Thus at the wellbore radius of 0.1 m gas mobility is reduced by a factor of 6540 and at a distance of 1 m by a factor 11,631. The relatively small value of power-law exponent n here (½) is similar to behavior observed in the "low-quality" foam regime (Alvarez et al., 2001). Like Rossen et al. (2011) we assume a particularly simple foam model here to illustrate the effects of shear-thinning rheology without the other complications of foam behavior.

References

Abacioglu, Y., Sebastian, H.M., Oluwa, J.B., 2009. Advancing Reservoir Simulation Capabilities for Tight Gas Reservoirs, Paper SPE 122793, Presented at the 2009 Rocky Mountain Petroleum Technology Conference. Denver, CO, 14–16 April 2009.

Alvarez, J.M., Rivas, H., Rossen, W.R., 2001. A unified model for steady-state foam behavior at high and low foam qualities. SPE J. 6, 325–333.

Babu, D.K., Odeh, A.S., Al-Khalifa, A.J., McCann, R.C., 1991. The relation between wellblock and wellbore pressures in numerical simulation of horizontal wells. SPE J. 3, 324–328.

Baylor, B.A., Maggard, J.B., Wattenbarger, R.A., 1990. Improved Calculation of Oil Production Response to Electrical Resistance Heating (ERH), Paper SPE 20482 Presented at the Annual Technical Conference and Exhibition. New Orleans, LA, September 23–26, 1990.

Boeije, C.S., Rossen, W.R., 2013. Fitting Foam Simulation Model Parameters to Data, Presented at the 17th European Symposium on Improved Oil Recovery. St. Petersburg, Russia, 16–18 April 2013.

Boeije, C.S., Rossen, W.R. Gas injection rate needed for SAG foam processes to overcome gravity override, SPE J., http://dx.doi.org/10.2118/166244-PA, in press.

Buckley, S.E., Leverett, M.C., 1941. Mechanism of fluid displacement in sands. Trans. AIME 146, 107–116.

Amit Chakma, A., Jha, K.N., 1992. Heavy-Oil Recovery From Thin Pay Zones by Electromagnetic Heating, Paper 24817 Presented at the Annual Technical Conference and Exhibition. Washington, DC, October 4–7, 1992.

Chen, G., Tehrani, D.H., Peden, J.M., 1995. Calculation of Well Productivity in a Reservoir Simulator (II), Paper SPE 29932 Presented at the International Meeting on Petroleum Engineering. Beijing, China, 14–17 November 1995.

Cheng, L., Reme, A.B., Shan, D., Coombe, D.A., Rossen, W.R., 2000. Simulating Foam Processes at High and Low Foam Qualities, Paper SPE 59287 Presented at the SPE/DOE Symposium on Improved Oil Recovery. Tulsa, OK, 3–5 April 2000.

Computer Modeling Group, STARS User's Guide, Version 2006. Calgary, Alberta, Canada.

Coombe, D.A., 2012. Personal communication.

Dogru, A.H., 2010. Equivalent wellblock radius for partially perforated vertical wells – part I: anisotropic reservoirs with uniform grids. SPE J. 4, 1028–1037.

Faisal, A., Bisdom, K., Zhumabek, B., Mojaddam Zadeh, A., Rossen, W.R., 2009. Injectivity and Gravity Segregation in WAG and SWAG Enhanced Oil Recovery, SPE 124197 Presented at the 2009 SPE Annual Technical Conference and Exhibition held in New Orleans, Louisiana, USA, 4–7 October 2009.

Falls, A.H., Musters, J.J., Ratulowski, J., 1989. The apparent viscosity of foams in homogeneous bead packs. SPE Reserv. Eng. 4, 155–164.

Fanchi, J.R., 1990. Feasibility of Reservoir Heating by Electromagnetic Irradiation, SPE Paper 20483 Presented at the Annual Technical Conference and Exhibition. New Orleans, LA, September 23–26, 1990.

Hirasaki, G.J., Lawson, J.B., 1985. Mechanisms of foam flow through porous media – apparent viscosity in smooth capillaries. SPE J. 25, 176–190.

Ibrahim, M., 2013. Development of New Well Index Equation for Fracture Wells, Paper SPE 164017, Presented at the SPE Middle East Unconventional Gas Conference and Exhibition. Muscat, Oman, 28–30 January 2013.

Khatib, Z.I., Hirasaki, G.J., Falls, A.H., 1988. Effects of capillary pressure on coalescence and phase mobilities in foams flowing through porous media. SPE Reserv. Eng. 3, 919–926.

Kloet, M.B., Renkema, W.J., Rossen, W.R., 2009. Optimal Design Criteria for SAG Foam Processes in Heterogeneous Reservoirs, SPE 121581 Presented at the 2009 SPE EUROPEC/EAGE Annual Conference and Exhibition. Amsterdam, The Netherlands, 8–11 June 2009.

Kovscek, A.R., Radke, C.J., 1994. Fundamentals of foam transport in porous media. In: Schramm, L. (Ed.), Foams: Fundamentals and Applications in the Petroleum Industry,. ACS Symposium Series No. 242. American Chemical Society, Washington DC, pp. 115–163.

Kuehne, D.L., Ehman, D.I., Emanuel, A.S., Magnani, C.F., 1990. Design and evaluation of a nitrogen-foam field trial. J. Pet. Techol. 42, 504–512.

Lake, L.W., Johns, R.T., Rossen, W.R., Pope, G.A., 2014. Fundamentals of Enhanced Oil Recovery. Society of Petroleum Engineers, Richardson, TX.

Latooij, C.A., 2012. Injectivity in Non-Newtonian Two-Phase Flow (B.Sc. thesis). BTA/PE/12-18, Delft University of Technology. Available from: ⟨http://repository.tudelft.nl/⟩.

Leeftink, T.N., 2013. Injectivity Errors in Simulation of Foam EOR (B.Sc. thesis). Delft University of Technology. Available from: ⟨http://repository.tudelft.nl/⟩

Martinsen, H.A., Vassenden, F., 1999. Foam-Assisted Water Alternating Gas (FAWAG) Process on Snorre, Presented at the EAGE European IOR Symposium. Brighton, U.K., 18–20 August 1999.

Mochizuki, S., 1995. Well Productivity for Arbitrarily Inclined Well, Paper SPE 29133 Presented at the 13th Symposium on Reservoir Simulation. San Antonio, U.S.A., 12–15 February 1995.

Namdar Zanganeh, M., Kam, S.I., LaForce, T.C., Rossen, W.R., 2011. The method of characteristics applied to oil displacement by foam. SPE J. 16, 8–23.

Namdar Zanganeh, M., Rossen, W.R., 2013. Optimization of foam EOR: balancing sweep and injectivity. SPE Reserv. Eval. Eng. 16, 51–59.

Mathias, S.A., Hardisty, P.E., Trudell, M.R., Zimmerman, R.W., 2009. Approximate solutions for pressure buildup during CO_2 injection in brine aquifers. Transp. Porous Med. 79, 265–284.

McMillan, B., Kumar, N., Bryant, S.L., 2008. Time-Dependent Injectivity During CO_2 Storage in Aquifers, Paper SPE 113937 Presented at the Symposium on Improved Oil Recovery. Tulsa, OK, 20–23 April 2008.

Noh, M., Lake, L.W., Araque-Martinez, A., 2007. Implications of coupling fractional flow and geochemistry for CO_2 injection in aquifers. SPE Reserv. Eval. Eng. 10, 406–414.

Orr, F.M., 2007. Theory of Gas Injection Processes. Tie-Line Publications, Holte, Denmark.

Osterloh, W.T., Jante, M.J., Jr. 1992. Effects of gas and liquid velocity on steady-state foam flow at high temperature. Paper SPE 24197 Presented at the SPE/DOE Enhanced Oil Recovery Symposium, Tulsa, OK, 22-24 April 1992.

Peaceman, D.W., 1978. Interpretation of well-block pressure in numerical reservoir simulation. SPE J. 18, 183–194.

Peaceman, D.W., 1983. Interpretation of well-block pressure in numerical reservoir simulation with non-square grid blocks and anisotropic permeability. SPE J. 23, 531–543.

Peaceman, D.W., 1993. Representation of a horizontal well in numerical reservoir simulation. SPE Adv. Technol. Ser. 1, 7–16.

Pickup, G.E., Jin, M., Mackay, E.J., 2012. Simulation of Near-Well Pressure Build-up in Models of CO_2 Injection, Paper B34 presented at the EAGE European Conference on the Mathematics of Oil Recovery. Biarritz, France, 10–13 September 2012.

Pizarro, J.O.S., Trevisan, O.V., 1990. Electrical heating of oil reservoirs: numerical simulation and field test results. J Pet. Technol., 1320–1326.

Pope, G.A., 1980. The application of fractional flow theory to enhanced oil recovery. SPE J. 10, 191–205.

Rossen, W.R., 1996. Foams in enhanced oil recovery. In: Prud'homme, R.K., Khan, S. (Eds.), Foams: Theory, Measurements and Applications. Marcel Dekker, New York, pp. 413–464.

Rossen, W.R., Boeije, C.S., 2013. Fitting Foam Simulation Model Parameters for SAG Foam Applications, Paper SPE 165282 presented at the SPE Enhanced Oil Recovery Conference. Kuala Lumpur, Malaysia, 2–4 July 2013.

Rossen, W.R., Ocampo-Florez, A.A., Restrepo, A., Cifuentes, Marin, J., 2014. Long-Time Diversion in SAG Foam Enhanced Oil Recovery From Field Data, SPE Paper 170809 Presented at the SPE Annual Technical Conference and Exhibition held in Amsterdam, The Netherlands, 27–29 October 2014.

Rossen, W.R., van Duijn, C.J., Nguyen, Q.P., Shen, C., Vikingstad, A.K., 2010. Injection strategies to overcome gravity segregation in simultaneous gas and water injection into homogeneous reservoirs. SPE J. 15, 76–90.

Rossen, W.R., Venkatraman, A., Johns, R.T., Kibodeaux, K.R., Lai, H., Moradi Tehrani, N., 2011. Fractional flow theory applicable to non-Newtonian behavior in EOR processes. Transp. Porous Med. 89, 213–236.

Rossen, W.R., Zeilinger, S.C., Shi, J.-X., and Lim, M.T., Simplified mechanistic simulation of foam processes in porous media, SPE J. 4, 279-287 (1999).

Rossen, W.R., Zhou, Z.H., 1995. Modeling foam mobility at the limiting capillary pressure. SPE Adv. Technol. 3, 146–152.

Schlumberger, 2010. ECLIPSE∗ Reservoir Simulation Software, Version 2010.2, Technical Description.

Schramm, L.L. (Ed.), 1994. Foams: Fundamentals and Applications in the Petroleum Industry, ACS Advances in Chemistry Series No. 242, American Chemical Society. Washington, DC.

Sharma, A., Delshad, M., Huh, C., Pope, G.A., 2011. A Practical Method to Calculate Polymer Viscosity Accurately in Numerical Reservoir Simulators, SPE 147239 Presented at the SPE Annual Technical Conference and Exhibition held in Colorado, Denver, USA, 31 October 2011–2 November 2011.

Shan, D., Rossen, W.R., 2004. Optimal injection strategies for foam IOR. SPE J. 9, 132–150.

Tang, G.Q., Kovscek, A.R., 2006. Trapped gas fraction during steady-state foam flow. Transp. Porous Med. 65, 287–307.

Xu, Q., Rossen, W.R., 2003. Effective viscosity of foam in periodically constricted tubes. Colloids Surf. A: Physicochem. Eng. Asp. 216, 175–194.

Zhou, Z.H., Rossen, W.R., 1995. Applying fractional-flow theory to foam processes at the 'limiting capillary pressure'. SPE Adv. Technol. 3, 154–162.